JAERI-M
87-190

A PARAMETER DIAGRAM FOR LOWER-HYBRID CURRENT DRIVE IN TOKAMAKS

November 1987

Kazuya UEHARA, Masahiro NEMOTO and Takashi NAGASHIMA

日本原子力研究所
Japan Atomic Energy Research Institute

JAERI-Mレポートは，日本原子力研究所が不定期に公刊している研究報告書です。
入手の問合わせは，日本原子力研究所技術情報部情報資料課（〒319-11茨城県那珂郡東海村）あて，お申しこしください。なお，このほかに財団法人原子力弘済会資料センター（〒319-11 茨城県那珂郡東海村日本原子力研究所内）で複写による実費頒布をおこなっております。

JAERI-M reports are issued irregularly.
Inquiries about availability of the reports should be addressed to Information Division Department of Technical Information, Japan Atomic Energy Research Institute, Tokai-mura, Naka-gun, Ibaraki-ken 319-11, Japan.

編集兼発行　日本原子力研究所
印　　刷　いばらき印刷㈱

JAERI-M 87-190

A Parameter Diagram for Lower-Hybrid Current Drive in Tokamaks

Kazuya UEHARA, Masahiro NEMOTO[+] and Takashi NAGASHIMA[++]

Department of JT-60 Facility
Naka Fusion Research Establishment
Japan Atomic Energy Research Institute
Naka-machi, Naka-gun, Ibaraki-ken

(Received October 19, 1989)

Parameters of lower-hybrid current driven tokamaks are phenomenologically surveyed using the relationships among mode conversion condition, the threshold condition for parametric instability and the accessibility condition. It is shown that the density limit obtained experimentally can be derived from the criteria $\omega_0/\omega_{LH} > x_0$ and $\omega_{pe}/\omega_{ce} < y_0$, where x_0 is determined by the mode conversion condition and y_0 is determined by threshold condition of parametric instability or the accessibility condition. The parameter space for lower-hybrid current drive in tokamaks is divided into two regions dominated by parametric instability and accessibility, respectively.

Keywords: Low-Hybrid Current Drive, Tokamak, Mode Conversion, Parametric Instability, Accessibility Condition, Density Limit

---

This work was performed in 1982 when one of the authors (M.N.) had stayed at plasma heating Laboratory in JAERI as a student fellow on leave from The Technological University of Nagaoka, Niigata, 949-54

+ Department of large Tokamak Research
++ Department of Thermonuclear Fusion Research

トカマクに於ける低域混成波電流駆動のパラメータダイヤグラム

日本原子力研究所那珂研究所JT－60試験部
上原　和也・根本　正博[+]・永島　孝[++]

（1987年10月19日受理）

低域混成波電流駆動トカマクの最適なパラメーターが，モード変換とパラメトリック不安定性及び近接性条件の関係式を用いてサーベイされている。実験的に得られている密度限界が，$\omega_0/\omega_{LH}>x_0$ 及び $\omega_{pe}/\omega_{ce}<y_0$ の規準で整理される。たゞしここに x_0 はモード変換の条件で決定されており，y_0 はパラメトリック不安定性の閾値の条件か又は近接性の条件のいずれかで決定される。電流駆動のパラメーター領域はパラメトリック不安定性が支配的な領域と近接性が支配的な領域との2つの領域に分けられることが示されている。

本研究は昭和57年度当時長岡科学技術大学在学中の根本正博氏が学生実習生として原研加熱工学第2研究室に派遣されていた時に行った研究をまとめたものである。

那珂研究所：〒311－02 茨城県那珂郡那珂町大字向山801－1
＋ 臨界プラズマ研究部
＋＋ 核融合研究部

Contents

目　　次

1. Introduction

Non-inductive current drive in a tokamak by rf travelling waves[1] would enable steady state operation of a tokamak as well as ramping-up of the plasma current[2,3], and finally the elimination of the OH transformer in a tokamak fusion reactor[4,5]. Among the methods of current drive by rf waves, namely the lower-hybrid wave[6], the ion cyclotron wave[7], the Alfvén wave[8,9] and the electron cyclotron wave[10], current drive by the lower hybrid wave is the only method which is confirmed experimentally[11,12] for large currents relevant to reactors. The lower-hybrid current driven tokamak has been discussed in connection with quasi-linear theory[13] as well as mode conversion theory[14] and parametric instability[15].

The quasi-linear theory can explain that the rf current is inversely proportional to the average density $\bar{n}_e$.[6] However, this theory cannot explain the fact that the density limit exists in most lower-hybrid current driven tokamaks and that the density limit is improved by increasing the driving frequency. It has been reported that this critical density is limited by nonlinear effects such as the parametric instabilities.[16,17] We notice the fact that successful current drive experiments at higher density are less efficient at lower magetic field[18] and more efficient at higher driving frequency ω_0 $(=2\pi f_0)$[19].

In this paper, we survey data from various lower hybrid current driven tokamaks using the criteria of mode conversion, parametric instability and accessibility. As a result, we propose a convenient parameter diagram that can be applied all current driven tokamaks.

In section 2, the condition to realize current drive is surveyed using verious experimental data, and in section 3 the parameter diagram for obtaining lower hybrid current drive is drawn. Finally, the discussion and summary are given in section 4.

2. Condition for Lower-hybrid Current Drive

There are some conditions that have to be satisfied to obtain successful current drive in tokamaks. Among them, the conditions that the plasma be free of mode conversion, or no turning point to exist in

1. Introduction

Non-inductive current drive in a tokamak by rf travelling waves[1] would enable steady state operation of a tokamak as well as ramping-up of the plasma current[2,3], and finally the elimination of the OH transformer in a tokamak fusion reactor[4,5]. Among the methods of current drive by rf waves, namely the lower-hybrid wave[6], the ion cyclotron wave[7], the Alfvén wave[8,9] and the electron cyclotron wave[10], current drive by the lower hybrid wave is the only method which is confirmed experimentally[11,12] for large currents relevant to reactors. The lower-hybrid current driven tokamak has been discussed in connection with quasi-linear theory[13] as well as mode conversion theory[14] and parametric instability[15].

The quasi-linear theory can explain that the rf current is inversely proportional to the average density $\bar{n}_e$.[6] However, this theory cannot explain the fact that the density limit exists in most lower-hybrid current driven tokamaks and that the density limit is improved by increasing the driving frequency. It has been reported that this critical density is limited by nonlinear effects such as the parametric instabilities.[16,17] We notice the fact that successful current drive experiments at higher density are less efficient at lower magetic field[18] and more efficient at higher driving frequency ω_0 $(=2\pi f_0)$[19].

In this paper, we survey data from various lower hybrid current driven tokamaks using the criteria of mode conversion, parametric instability and accessibility. As a result, we propose a convenient parameter diagram that can be applied all current driven tokamaks.

In section 2, the condition to realize current drive is surveyed using verious experimental data, and in section 3 the parameter diagram for obtaining lower hybrid current drive is drawn. Finally, the discussion and summary are given in section 4.

2. Condition for Lower-hybrid Current Drive

There are some conditions that have to be satisfied to obtain successful current drive in tokamaks. Among them, the conditions that the plasma be free of mode conversion, or no turning point to exist in

the plasma, and the small collisionality are probably necessary. The former item requires relatively lower density of the plasma, and the latter the relatively higher electron temperature or large phase velocity of the wave. In the final stationary state of the electron distribution function, the quasi-linear diffusion due to the presence of rf power balances the collisional relaxation between high energy electrons and bulk electrons.

Experimental results in most lower hybrid current drive tokamaks show that the driving current is inversely proportional to $\bar{n}_e$ and disappears above a certain critical density. In JFT-2, the rf current disappears completely above the density of 7×10^{12} cm^{-3} as shown in Fig. 1, at the same time the parametric decay wave grows to be large amplitude as shown in Fig. 2. So it is natural to consider that the threshold of parametric instability determines one of the conditions of the critical density of current drive as shown by the MIT[17-19] and Grenoble[20] groups. On the other hand, the ASDEX team reports another experimental condition of LHCD, where the rf current is still flowing although the parametric dexay waves still grow, and the rf current does not disappear suddenly with an increase of the density.[21] The ASDEX result indicates that the critical density does not coincide the onset condition of parametric decay instability. It seems in this case that the critical density is determined by the accessibility condition. This should result in a more gradual deterioration of the current drive efficiency. Considering these facts, we search possible parameter space for efficient lower hybrid current drive with the following conditions : $\omega_0/\omega_{LH}(0) > x_0$, growth rate $\gamma < \gamma_c$ and $n_z > n_{za}$, where $\omega_{LH}(0)$ is lower hybrid frequency at the center, x_0 is constant value to be determined by the mode conversion condition, γ_c is the experimental growth rate of the parametric instability and n_{za} is lower limit of the parallel refractive index that satisfies the accessibility, which should be determined by Brambilla spectrum. The accessibility condition can not be satisfied when the density is large.

3. Parameter Diagram for Current Drive

3.1 Parameter diagram

If we define $x = \omega_0/\omega_{LH}(0)$ and $y = \omega_{pe}/\omega_{ce}$, x and y are combined to an equation:

$$4.41 \times 10^4 f_0^{-2} \bar{n}_e (b\mu)^{-1} z_e^2 x^2 = 1 + y^2 \qquad (1)$$

where ω_{pe} is electron plasma frequency, ω_{ce} is electron cyclotron frequency, μ is ion mass number, z_e is effective charge state, f_0 is driving frequency in Hz, $\bar{n}_e$ is the line average density in cm^{-3} and b is the ratio of $\bar{n}_e$ to the central density n_{e0}, i.e., $\bar{n}_e = bn_{e0}$, $0 < b < 1$. Here we assume that plasma contains only a single species of ions. The value of b is determined by the radial density profile. Equation (1) gives a hyperbola on a x-y cartesian coordinate system with $y = +(210/f_0)\sqrt{\bar{n}_e/b}\ x$ and $y = -(210/f_0)\sqrt{\bar{n}_e/b}\ x$ as asymptotic lines. At first, the condition that the mode conversion does not occur in the plasma is expressed as

$$x \geq x_0 \qquad (2)$$

in this parameter diagram.

We add the conditions of accessibility and parametric instability to this diagram as a lower hybrid current drive criterion. The accessibility condition is expressed as ; $n_z > n_{za} = \sqrt{K_{//}} + K_x/\sqrt{K_\perp}^{22})$, where n_z is the parallel refractive index of the lower-hybrid wave, n_{za} is the critical n_z, which is determined by Brambilla spectrum, and $K_{//} = 1-(\omega_{pi}/\omega_0)^2-(\omega_{pe}/\omega_0)^2$, $K_\perp = 1-\omega_{pi}^2/(\omega_0^2-\omega_{ci}^2)-\omega_{pe}^2/(\omega_0^2-\omega_{ce}^2)$, $K_x = -\omega_{pi}^2\omega_{ci}/(\omega_0^2-\omega_{ci}^2)\omega_0-\omega_{pe}^2\omega_{ce}/(\omega_0^2-\omega_{ce}^2)\omega_0$. This condition can be expressed on the x-y plane as

$$y \leq y_{Ac}\ (x,\ n_{za},\ \bar{n}_e) \qquad (3)$$

The value of y_{Ac} $(x,\ n_{za},\ \bar{n}_e)$ is a function of x, n_{za} and $\bar{n}_e$ if we give a constraint to the values of f_0, b, μ and z_e. As shown later, it may occur that current drive is limited by the accessibility parameter.

In JFT-2 and Alcator-C. The critical density is observed when the nonresonat parametric instability becomes active. We remark that Liu

et al, have attempted to explain the density limit theoretically by the resonant type of parametric instability[23], however, we apply the experimental data rather than theoretical one. Using the data of JFT-2 [24,25] and Alcator-C[17], we estimate that $\gamma \propto T_{es}^{-1.55}\bar{n}_e^{2.08}B_t^{-3.45}$ as the growth rate of non-resonant decay waves, which is similar to a theoretical one, $\gamma \propto T_e^{-1}\bar{n}_e B_t^{-2}$ [20], where T_{es} is edge electron temperature, T_e is central electron temperature and B_t is toroidal field. The density and temperature profile are assumed to vary as $(1 - (r/1.08a)^2)^2$, which is emprically found in JFT-2 and the edge electron temperature is obtained at r = a. In JFT-2, the parametric decay wave grows to a significant level when $\bar{n}_e$ increases above 7×10^{12} cm^{-3} at T_e = 550 eV and B_{t0} = 12.5 kG and the current drive effect disappears simultaneously as shown in Figs. 1 and 2. If we assume that the experimental threshold of parametric instability is determined when γ is larger than a critical value of γ_c, the stabilization condition of the nonresonant parametric inctability can be expressed as $\gamma < \gamma_c$, which should yield the possible region on the x-y plane by

$$y \leq y_{PI}\ (x,\ T_e,\ \bar{n}_e) \qquad (4)$$

The value of y_{PI} (x, T_e, $\bar{n}_e$) indicates that a function of x, T_e and $\bar{n}_e$ if we give a constraint to the values of f_0, b, μ, z_e and γ_c. This condition is that the rf power should not be dissipated to the decay wave. In other words, in the parameter region that this condition is not satisfied, the rf power for the current drive is deprived by the parametric instability. From these considerations we consider that the possible current drive parameters can be searched in a certain region on the x-y plane determined by eqs.(2), (3) and (4).

3.2 Critical density

In Fig. 3, JFT-2 current drive diagram is graphically expressed with an aid of computer using eqs.(1), (2), (3) and (4) with $\bar{n}_e$ as a parameter, where $\gamma_c = 8 \times 10^{10}$, x_0 = 1.84, n_{za} = 2.1 and T_e = 550 eV were used in eq.(4), where γ_c is expressed in the unit T_e ; eV, B_t ; Gauß, $\bar{n}_e$; cm^{-3} and $n_z > n_{za}$ (=2.1) corresponds that about 70-80% of rf power enters into the plasma center. In general, the current drive should always be possible when all conditions of accessibility, mode conversion

and no parametric instability, in which all power is dissipated to the electron Landau damping to yield the rf current are satisfied. This condition is ; $x > x_0$, $y < y_{Ac}$ and $y < y_{PI}$ as shown by shadow region in Fig. 3. However, we consider as a critical density of the current drive in the following. The current drive is possible if there exists some power to be dissipated by electron Landau damping, that is, the current drive is possible unless the rf power is lost completely by the parametric decay waves or non accessibility. This condition is ; $x > x_0$ and either $y < y_{PI}$ or $y < y_{Ac}$. When the condition of $y_{AC} < y < y_{PI}$ is available, a part of the accessibility condition is not satisfied and rf power for current drive is reduced to some extent, however, the rf current is still generated by the residual accessible power that is not yet deprived by the decay waves. On the other hand, when the condition of $y_{PI} < y < y_{AC}$ occurs, the parametric instability already occurs and the rf power for current drive is reduced in some extent. However, the rf current is still generated by the residual power that exists in the plasma which satisfies the accessibility condition. From this point of view, there exists two cases depending on machine parameters for the critical density of current drive. Ths former case occurs when x_0 is larger than the intersection point of $y = y_{PI}(x)$ and $y = y_{Ac}(x)$ as shown in JFT-2. In this case, the critical density is defined at $x = x_0$ and $y = y_{PI}(x_0)$. As shown in Fig. 3, the constraint on accessibility condition is more restrictive than the parametric condition. This case indicates that the accessibility is sacrified in some extent, however, the parametric instability does not occur. In this case, it can say that the critical parameter of the current drive is limited by the parametric instability. So, this case may be called as the parametric dominant region. However, also in this case the current drive effect disappears completely when there exists no power on the rf spectrum with increase of n_{za}. In JFT-2, the intersection point of $y = y_{PI}(x)$ and $x = 1.84$ is $y = 1.08$, and the predicted critical density $\bar{n}_{ecT}$ is estimated to be $\bar{n}_{ecT} = 6.5 \times 10^{12}$ cm^{-3}. The latter case occurs when x_0 is smaller than the intersection point of $y = y_{PI}(x)$ and $y = y_{Ac}(x)$. In this case, the critical density is defined at $x = x_0$ and $y = y_{Ac}(x_0)$. The constraint on the parametric instability is more restrictive than the accessibility condition in this case. This case indicates that the parametric instability is sacrified, however, the accessibility condition is still satisfied. Thus, it can be said that the critical parameter of

current drive is limited by the accessibility. This may be called as the accessibility dominant region, which corresponds ASDEX case. In this case the critical $n_z > n_{za}$ is estimated to be 30-40% of the rf spectrum. We can obtain $\bar{n}_{ecT}$ numerically with an aid of computer by substituting eq.(3) or eq.(4) into eq.(1) and eliminating B_{t0} and y, which are

$$4.41 \times 10^4 f_0^{-2}(b\mu)^{-1} z_e^2 x_0^2 = b\bar{n}_{ecT}^{-1} + 1.024 \times 10^{-5} \bar{n}_{ecT}^{-1} \dot{T}^{20} \gamma_c^{0.578} T_e^{0.904} \quad (5)$$

for the parametric dominat region ($y_{PI} > y_{AC}$), which corresponds the higher electron temperature or the small n_{za} case, and we can obtain $\bar{n}_{ecT}$ using eqs.(2) and (3) for the accessibility dominant case ($y_{AC} > y_{PI}$), which corresponds for lower electron temperatures or large n_{za}. It should be noted that $\bar{n}_{ecT}$ increases with increasing f_0, n_{za} and T_e, and that there exist two cases that either the accessibility or the parametric instability is dominant, depending on the values of n_{za} and T_e. In Table 1, we summarize various cases of current drive machines, in which n_{za}, x_0, y_0, y_{AC}, y_{PI}, the experimental critical density $\bar{n}_{ecx}$ and $\bar{n}_{ecT}$ that can be estimated using this criterion are included, and n_{max} is the upper limit of rf spectrum. The dominant parameter causing the density limit is also listed in Table 1.

The values of $\bar{n}_{ecT}$ vs f_0 for the parametric dominant parameter and for the accessibility dominant parameter are shown in Figs. 4 and 5, respectively, in which are contained tha $\bar{n}_{ecx}$ by closed circles and the predicted one are shown by straight lines. Similarly to the frequency dependence, the value of $\bar{n}_{ecT}$ increases with increasing B_{t0}, n_{za} and T_e. As shown in Figs. 4 and 5, the value of $\bar{n}_{ecx}$ fit well with the predictions except for several examples.

3.3 Application to future tokamak

There are a few machines where the parametric parameter dominants due to relatively low electron temperatures which do not to enough to suppress the parametric instability in present parameters of lower hybrid tokamaks. The density limit in future machines with reletively higher T_e will be mostly in the parametric dominant region as long as there exists some rf power to satisfy the accessibility condition. Whether

the parametric instability is dominant or the accessibility is dominant can obtain from the conditions that $x = x_0$ and $y_{PI} = y_{AC}$ in eqs.(3) and (4). JT-60 LHCD case is shown in both parametric dominant and accessibility dominant parameters in Fig. 6. When $T_e = 0.8$ keV and $n_{za} = 1.3$, then $y_{AC} = 0.9 > y_{PI}$, which is accessibility dominant case, $\bar{n}_{ecT} = \bar{n}_{ecAc} = 2.9 \times 10^{13}$ cm^{-3} and when $T_e = 2$ keV and $n_{za} = 1.3$ then $y_{PI} = 1.2 > y_{AC}$, which is parametric dominant case, the constraint of parametric instability is enlarged to be $\bar{n}_{ecT} = \bar{n}_{ecPI} = 4.9 \times 10^{13}$ cm^{-3}. Such behaviour for the case of JT-60 is shown in Fig. 7, in which the value of $\bar{n}_{ecT}$ is shown against T_e with the frequency as a parameter. The value of $\bar{n}_{ecT}$ is plotted against T_e. When T_e is lower than a critical value, which is shown by arrows, the critical density is limited by the normal accessibility and when T_e is larger than a critical one, $\bar{n}_{ecT}$ is improved by increase of T_e. When n_{za} becomes large $\bar{n}_{ecT}$ is improved, however, $\bar{n}_{ecT}$ cannot be beyond the upper limit on n_{za} which is determined by the upper limit of the rf spectrum, that is, there is no power value n_{za} of the rf spectrum.

4. Discussion and Conclusions

The physical effect of $\omega_0/\omega_{LH} > x_0$ and $\gamma > \gamma_c$ is different in general, that is, the former is condition of mode conversion and/or of the interaction to ions lower hybrid wave, and the latter is the threshold condition of the parametric instability. In the parameter diagram discussed here, the possible current drive parameter is defined by the relation of x and y with an aid of the constraint condition of mode conversion, parametric threshold and the accessibility.

Recent experiments on Versator-II indicate that a higher value of $\bar{n}_{ecX}$ was obtained by using a higher frequency without increasing B_{t0}. This case seems to correspond to the accessibility dominant case. In the Versator-II case,[19] the non accessible part of the rf spectrum is estimated to be more than 50% of total since n_{za} becomes relatively large, that is, the density limit is improbed as long as the accessibility condition is satisfied. The term of B_t is not included in eq.(5). In this sense f_0 is independent of B_{t0}. Both the Versator and Kyoto experiments[19,30] were in accessibility dominant regime due to low T_e.

the parametric instability is dominant or the accessibility is dominant can obtain from the conditions that $x = x_0$ and $y_{PI} = y_{AC}$ in eqs.(3) and (4). JT-60 LHCD case is shown in both parametric dominant and accessibility dominant parameters in Fig. 6. When $T_e = 0.8$ keV and $n_{za} = 1.3$, then $y_{AC} = 0.9 > y_{PI}$, which is accessibility dominant case, $\bar{n}_{ecT} = \bar{n}_{ecAc} = 2.9 \times 10^{13}$ cm^{-3} and when $T_e = 2$ keV and $n_{za} = 1.3$ then $y_{PI} = 1.2 > y_{AC}$, which is parametric dominant case, the constraint of parametric instability is enlarged to be $\bar{n}_{ecT} = \bar{n}_{ecPI} = 4.9 \times 10^{13}$ cm^{-3}. Such behaviour for the case of JT-60 is shown in Fig. 7, in which the value of $\bar{n}_{ecT}$ is shown against T_e with the frequency as a parameter. The value of $\bar{n}_{ecT}$ is plotted against T_e. When T_e is lower than a critical value, which is shown by arrows, the critical density is limited by the normal accessibility and when T_e is larger than a critical one, $\bar{n}_{ecT}$ is improved by increase of T_e. When n_{za} becomes large $\bar{n}_{ecT}$ is improved, however, $\bar{n}_{ecT}$ cannot be beyond the upper limit on n_{za} which is determined by the upper limit of the rf spectrum, that is, there is no power value n_{za} of the rf spectrum.

4. Discussion and Conclusions

The physical effect of $\omega_0/\omega_{LH} > x_0$ and $\gamma > \gamma_c$ is different in general, that is, the former is condition of mode conversion and/or of the interaction to ions lower hybrid wave, and the latter is the threshold condition of the parametric instability. In the parameter diagram discussed here, the possible current drive parameter is defined by the relation of x and y with an aid of the constraint condition of mode conversion, parametric threshold and the accessibility.

Recent experiments on Versator-II indicate that a higher value of $\bar{n}_{ecX}$ was obtained by using a higher frequency without increasing B_{t0}. This case seems to correspond to the accessibility dominant case. In the Versator-II case,[19] the non accessible part of the rf spectrum is estimated to be more than 50% of total since n_{za} becomes relatively large, that is, the density limit is improbed as long as the accessibility condition is satisfied. The term of B_t is not included in eq.(5). In this sense f_0 is independent of B_{t0}. Both the Versator and Kyoto experiments[19,30] were in accessibility dominant regime due to low T_e.

If y_0 were increased to the allowed level concomitant to the increase in f_0 the critical density should increase further. It should be noted that the condition for the critical density must incorporate the condition on B_t as well as f_0 as given by eqs.(3) and (4), which seems to support the current drive experiment at the higher density region with reletively high B_t and/or higher f_0 in Versator-II[19] and in Alcator-C[18].

In this paper, we refer the experimental scaling law for the growth rate of parametric instability that is obtained in only two machines of JFT-2 and Alcator-C. However, we can refine the criterion for current drive if we use a more precise expression for the proper threshold of each machine itself. The conditions on the parametric instability and the accessibility may be more stringent as well as the condition for no turning point to exist. The switch over condition from ions from electrons suggested by the NET group as the criterion of the current drive[33] seems to be included in the condition that no mode conversion exists in plasmas. It was also recognized in another paper that the non-resonant parametric instability is more dominant over the resonant type during lower-hybrid current drive.

It is noted that the critical density for current drive is defined when rf power is thoroughly lost due to the deterioration of the accessibility and the occurrence of the parametric instability. How is n_{za} defined? In general, n_{za} is defined by the parameters that rf power can propagate to the plasma center. For the parametric dominant case the part of $n_z > n_{za}$ is estimated to be 70-80% of the total power, that is, the only accessibility condition is violated in this ragion and the residual power to be useful for the current drive is 70-80% of the total rf power, which is dissipated by both decay waves and the non accessible part of the rf spectrum until the current drive effect disappears with increasing of $\bar{n}_e$. For the accessibility dominant case, the part of $n_z > n_{za}$ is about 30-40% of the total power, that is, the parametric instability already dissipates most of rf power in this case and the residual power to be useful for the current drive is only 30-40%. This power is disipated by decay waves as well as the non accessible part of the rf spectrum until the current drive effect disappears with increase of $\bar{n}_e$.

The differences in b and consequently in $\omega_0/\omega_{LH}(0)$, from tokamak to tokamak may be due to differences in current drive. These may be considered to be one of the reasons why the deviation of $\bar{n}_{ecT}$ to $\bar{n}_{ecX}$

occurs.

We can deduce the dependence of the critical density on frequency and toroidal magnetic field observed in many current drive experiments by the parameter diagram described in this paper, and we can add other parameters to the criterion for current drive, namely, the electron temperature and the citical n_{za}. When the electron temperature becomes large parametric instability is effectively suppressed and the critical density increases. When the critical n_{za} becomes larger the critical density is improved although the magnitude of the rf current becomes small until the rf power for the current drive disappears completely due to no accessibility. One can search for possible current drive parameters in each machine if appropriate constraint conditions of x_0, y_0, n_{za}, T_e and so on are substituted to eqs.(1) to (4).

In conclusion, we can examine the density limit for lower-hybrid current driven in tokamaks using the parameter diagram which incorporates the growth rate of the non-resonant parametric instability and the accessibility condition. The frequency dependence of the critical density observed in many current drive machines can be predicted using the parameter diagram.

Acknowledgments

Fruitful discussion with Drs. T. Yamamoto, K. Sakamoto and our colleague in Plasma Heating Laboratory II of JAERI are greatly appreciated. We also express our thanks to Drs. H. Shirakata, M. Yoshikawa, K. Tomabechi, Y. Iso and S. Mori for their continuous encouragement throughout this research. Useful criticism and reading manuscript in English grammer are greatly appreciated to Dr. J. Stevens.

occurs.

We can deduce the dependence of the critical density on frequency and toroidal magnetic field observed in many current drive experiments by the parameter diagram described in this paper, and we can add other parameters to the criterion for current drive, namely, the electron temperature and the citical n_{za}. When the electron temperature becomes large parametric instability is effectively suppressed and the critical density increases. When the critical n_{za} becomes larger the critical density is improved although the magnitude of the rf current becomes small until the rf power for the current drive disappears completely due to no accessibility. One can search for possible current drive parameters in each machine if appropriate constraint conditions of x_0, y_0, n_{za}, T_e and so on are substituted to eqs.(1) to (4).

In conclusion, we can examine the density limit for lower-hybrid current driven in tokamaks using the parameter diagram which incorporates the growth rate of the non-resonant parametric instability and the accessibility condition. The frequency dependence of the critical density observed in many current drive machines can be predicted using the parameter diagram.

Acknowledgments

Fruitful discussion with Drs. T. Yamamoto, K. Sakamoto and our colleague in Plasma Heating Laboratory II of JAERI are greatly appreciated. We also express our thanks to Drs. H. Shirakata, M. Yoshikawa, K. Tomabechi, Y. Iso and S. Mori for their continuous encouragement throughout this research. Useful criticism and reading manuscript in English grammer are greatly appreciated to Dr. J. Stevens.

References

1) D.J. Wort; Plasma Phys. 13 (1971) 253
2) F. Jobes, J. Stevens, R. Bell, S. Bernabei, A. Cavallo, T.K. Chu, S. Cohen, B. Denne, P. Efthimion, E. Hinnov, W. Hooke, J. Hosea, E. Mazzucato, R. McWilliams, R. Motley, S. Suckewer, G. Taylor, J. Timberlake, S.von Goeler and R. Wilson; Phys. Rev. Lett. 55 (1984) 1005
3) H. Leuterer, D. Eckhartt, H. Söldner, G. Becker, K. Bernhardi, M. Brambilla, Brinkschulte, H. Derfler, U. Ditte, A. Eberhagen, G. Fussmann, O. Gehre, J. Gerkei, J. Gernhardt, G.von Gierke, E. Clock, O. Gruber, G. Hass, M. Hesse, G. Janeschitz, K. Karger, M. Keilhacker, S. Kissel, O. Kluber, M. Kornherr, G. Lisitano, R. Magne, H.M. Mayer, K. McCormick, D. Meisel, V. Mertens, E.R. Muller, M. Munich, H. Murmann, . Poschenrieder, H. Rapp, F. Ryter, K.H. Schmitter, F. Schneider, G. Siller, P. Smeulders, K.H. Steuner, T. Vien, F. Wagner, F.V. Woyna and M. Zouhar; Phys. Rev. Lett. 55 (1985) 75
4) F.C. Jobes, S. Bernabei, T.K. Chu, W.M. Hooke, E.B. Meservey, R.M. Motley, J.E. Stevens and S.von Goeler; Phys. Rev. Lett. 55 (1985) 1295
5) K. Toi, K. Ohkubo, K. Kawahata, Y. Kawasumi, K. Matsuoka, N. Noda, Y. Ogawa, K. Sato, S. Tanahashi, T. Tetsuka, E. Kako, S. Hirokura, Y. Taniguchi, S. Kitagawa, Y. Hamada, J. Fujita and K. Matsuoka; Phys. Rev. Lett. 52 (1984) 2144
6) N.J. Fisch; Phys. Rev. Lett. 41 (1978) 873
7) N.J. Fisch; Nucl Fusion 21 (1981) 15
8) N.J. Fisch and C.F.F. Karne; Fluids 24 (1981) 27
9) H. Klima; Plasma Phys. 15 (1973) 1031
10) C.F.F. Karney and N.J. Fisch; Nucl. Fusion 21 (1981) 1549
11) T. Yamamoto, T. Imai, M. Shimada, N. Suzuki, M. Maeno, S. Konoshima, T. Fujii, K. Uehara, T. Nagashima, A. Funahashi and N. Fujisawa; Phys. Rev. Lett. 45 (1980) 719
12) S. Bernabei, C. Daughney, P. Efthimion, P. Hooke, J. Hosea, F. Jobes, A. Martin, E. Mazzucatto, E. Meservey, R. Motley, J. Stevens, S.von Goeler and R. Wilson; Phys. Revl Lett. 49 (1982) 1255
13) A.A. Vedenov; J. Nucl. Energy C5 (1963) 169
14) S.H. Stix; Phys. Rev. Lett. 15 (1965) 878
15) M. Porkolab; Phys. Fliuds 17 (1974) 1432

16) T. Yamamoto; in Non-Inductive Current Drive in Tokamaks Vol1, Chulham Laboratory, Abington, Euratom/UKAEA Association (Proc. Tech. Comittee Meeting, Culham, April, 1983)

17) M. Takase, M. Porkolab, J.J. Schuss, R.J. Watterson, C.L. Fiore, R.E. Slusher and C.M. Surko; Phys. Fliuds 28 (1985) 985 and Phys. Rev. Lett. 53 (1984) 1229

18) M. Porkolab, J.J. Schuss, B. Lloyd, Y. Takase, S. Texter, P. Bonoli, C. Fiore, . Gandy, D. Gwinn, B. Lipschultz, E. Marmar, D. Pappas, R. Parker and P. Pribyl; Phys. Rev. Lett. 53 (1984) 450

19) M.J. Mayberry, M. Porkolab, K.I. Chen, A.S. Fisher, D. Griffin, R. D. Kaplan, S.C. Luckhardt, J. Ramos and R. Rohatgi; Phys. Rev. Lett. 19 (1985) 829

20) Van Houtte, G. Brifford, P. Chabert, C. Gormezano, C. How, G. Ichtchenko, G. Melin, G. Moulin, F. Parlange and J.C. Vallet; Nucl. Fusion 24 (1984) 1485

21) F.X. Söldner, M. Brambilla, F. Leuterer and M. Munch, Report of Max-Planck Institute for Plasma Physics, IPP III/111, May 1986.

22) A. Bers; Proc. 3rd Topical conf. on RF Plasma Heating, paper a1, 1978

23) C.S. Liu, V.K. Tripathi, V.S. Chan and V. Stefan; Phys. Fluids 27 (1984) 1709

24) K. Uehara, H. Takeuchi, T. Imai, T. Yamamoto, T. Fujisawa and T. Nagashima; J. Phys. Soc. Jpn. 49 (1980) 2364

25) K. Uehara, T. Yamamoto, T. Fujii, N. Suzuki, T. Imai, S. Iizuka, H. Takeuchi, S. Kasai, H. Yoshida, N. Fujisawa and T. Nagashima; J. Phys. Soc. Jpn. 51 (1982) 1958

26) M. Porkolab; Nucl. Fusion 18 (1978) 367

27) S.C. Luckhardt, M. Porkolab, S.F. Knowlton, K.I. Chen, A.F. Fisher, A.S. Fisher, FS. McDermott and M. Mayberry; Phys. Rev. Lett. 48 (1982) 152

28) K. Ohkubo, S. Takamura, K. Kawahata, T. Tetsuka, N. Noda, K. Sakurai, S. Tanahashi, S. Takahashi and J. Fujita; Nucl. Fusion 22 (1982) 203

29) C. Gormerzano, P. Blanc, M.EL Shaer, W. Hess and G. Ichtchenko; in Proc. 3rd Varenna-Grenoble Int. Symp. on Heating in Toroidal Plasmas Grenoble 1982, Vol.II p.485

30) K. Nakamura, T. Maekawa, H. Terumichi, T. Cho and S. Tanaka; Phys. Rev. Lett. 47 (1981) 1902

31) V. Eudnikov, G. Gerasimenko, V.V. Dyachenko, L.A. Esipov, A.N.

Levitskii, A.A. Obukhov, I.P. Pavlov, A.Yu. Stepanov, I.E. Sakharov, S.V. Shatalin and O.N. Shcherbinin; Sov. J. Plasma Phys. 10 (1984) 281

32) F. Alladio, E. Barbato, C. Bardotti, G. Bracco, R. Bartiromo, G. Buceti, P. Buratti, F. Crisanti, R.De Angellis, F. Marco, M.De Pretis, D. Frigione, R. Giannella, M. Grolli, A. Mankuso, G. Mazzitelli, F. Orsitto, V. Pericoli, L. Pieromi, S. Podda, G.B. Righetti, F. Romanelli, F. Santini, S.E. Segre, A.A. Tuccillo and V. Zanza; Nucl. Fusion 24 (1984) 725

33) J.G. Wegrowe and H. Engelman; Comment on Plasma Phys. Cont. Nucl. Fusion 8 (1984) 211

Table 1 Parameters during current drive in various tokamaks. Parentheses in each machine are the number of references.

	b	B_{to} (T)	T_e (keV)	f_o (GH_z)	n_{za}	n_{max}	x_o	y_o	y_{AC}	y_{PI}	$\bar{n}_{ecx}$ ($\times 10^{12} cm^{-3}$)	$\bar{n}_{ecT}$ ($\times 10^{12} cm^{-3}$)	gas	Dominant Region
JFT-2 [16]	0.4	1.25	0.55	0.75	2.1	8	1.84	0.992	0.95	0.99	6.0	6.5	D_2	P.I
VERSATOR-II [27]	0.575	0.8	0.28	0.8	2.8	15.4	1.93	1.294	1.36	0.7	6.0	6.4	H_2	A.C
VERSATOR-II [19]	0.575	1.01	0.14	2.45	3.8	4.6	4.19	1.871	1.79	0.56	20.0	18.7	H_2	A.C
JIPPT-II [28]	0.575	1.27	0.4	0.8	2.0	4	1.4	0.941	1.0	0.76	8.0	8.6	H_2	A.C
WEGA [29]	0.575	2.25	0.55	0.8	1.6	3.7	1.28	0.75	0.75	0.76	16.0	16.1	D_2	P.I
PLT [12]	0.4	3.1	1.0	0.8	1.4	4.2	1.55	0.386	0.54	1.16	8.0	11.4	D_2	P.I
WT-II [30]	0.575	1.3	0.035	0.915	2.4	8	1.72	0.796	1.16	0.29	6.0	8.7	H_2	A.C
FT-2 [31]	0.4	2.5	0.4	0.915	1.4	3.5	1.17	0.906	0.76	0.78	20.0	17.8	D_2	P.I
PETULA-B [20]	0.575	2.8	0.83	1.3	1.7	4	1.79	0.675	0.69	0.85	20.0	23.7	D_2	P.I
FT [32]	0.4	8.0	1.1	2.45	2.0	3	2.08	0.334	0.85	0.93	40.0	46.6	D_2	P.I
ALCATOR-C [18]	0.4	10.0	1.3	4.6	2.0	2.5	1.8	0.422	0.89	0.95	100.0	113.2	H_2	P.I
ASDEX [21]	0.575	2.5	1.5	1.3	2.3	2.8	1.9	0.95	0.95	0.92	23.0	23	D_2	A.C

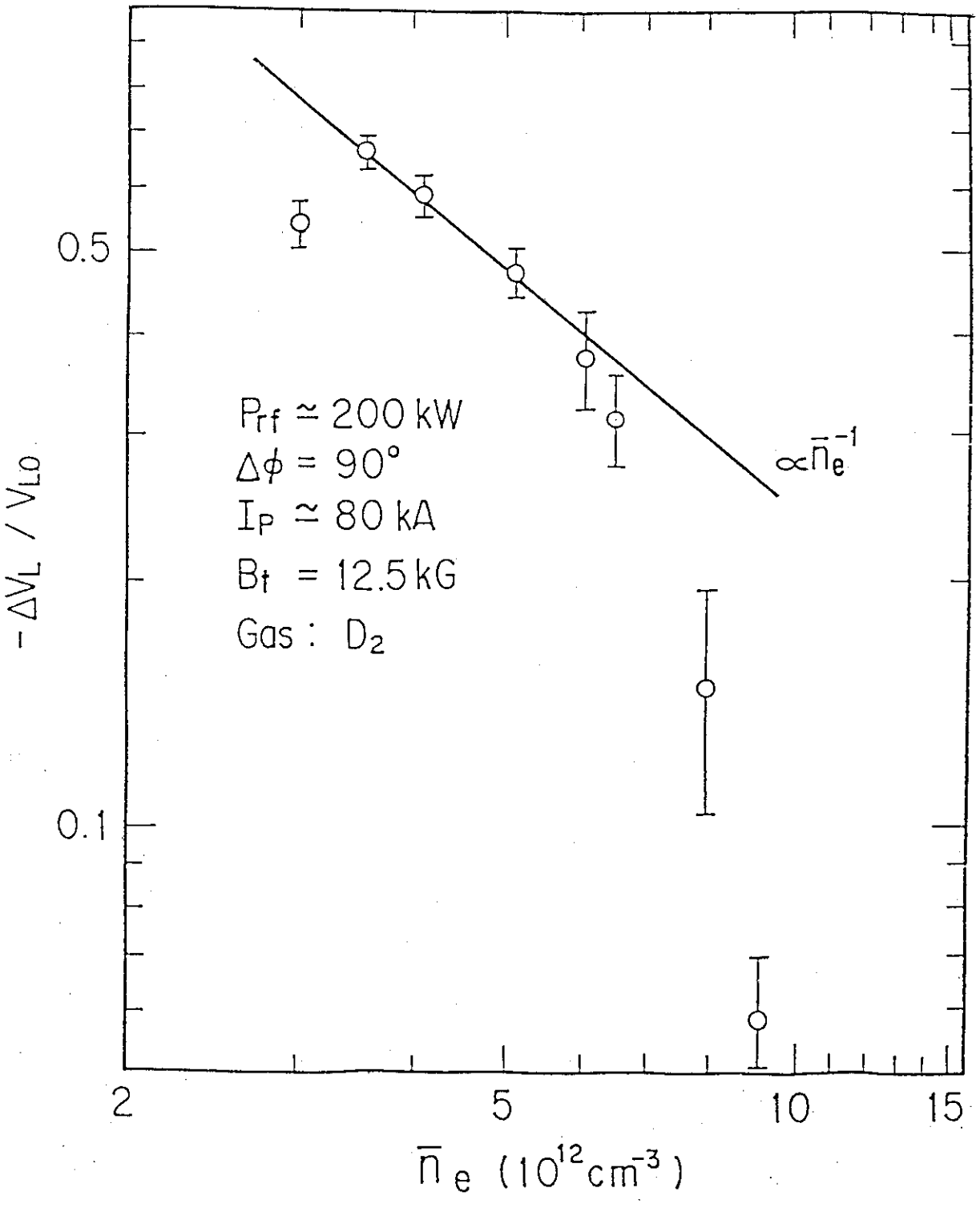

Fig. 1 JFT-2 current drive experiment is shown against the average plasma density $\bar{n}_e$. The drop rate of the loop voltage indicates that the rf current generated disappears when $\bar{n}_e$ is above 7×10^{-12} cm^{-3}.

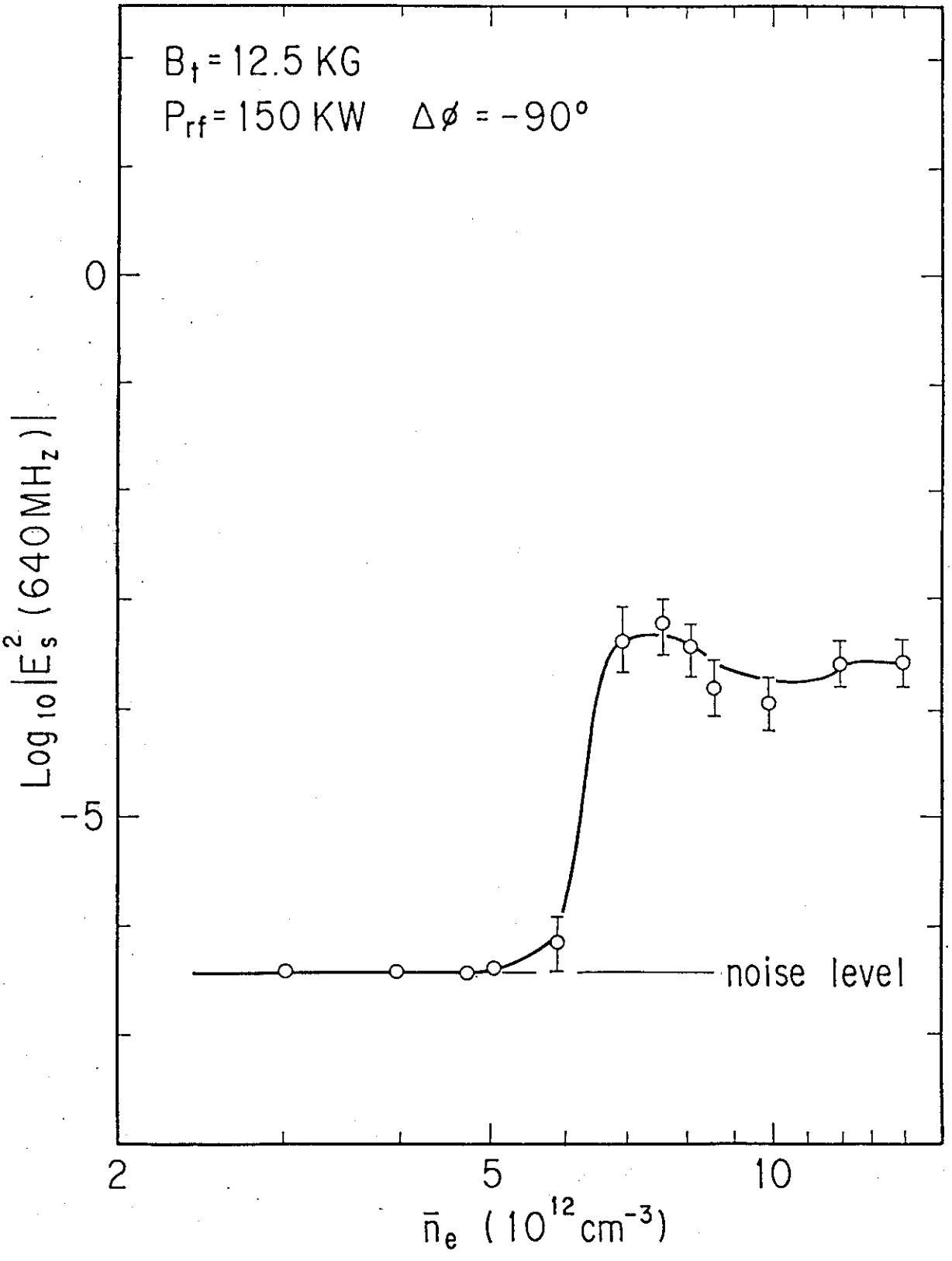

Fig. 2 The amplitude of the decay wave (640 MHz) picked up by an electrostatic probe is shown against the average density in JFT-2.

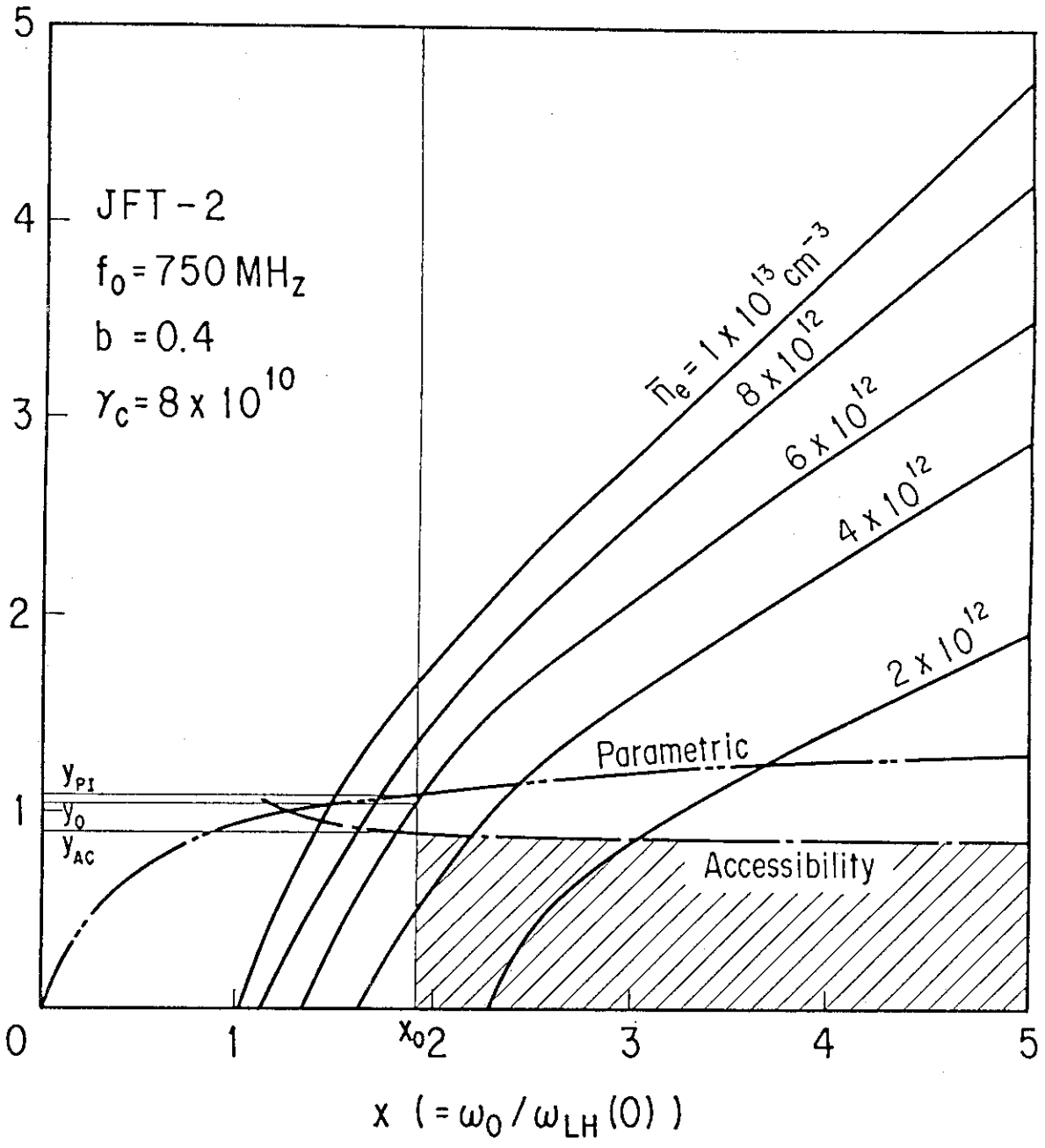

Fig. 3 The $x = \omega_0/\omega_{LH}(0)$ vs $y = \omega_{pe}/\omega_{ce}$ diagram for JFT-2 with the average density as a parameter, where we have added the accessibility y_{AC} (n_{za}=2.1) and the parametric instability y_{PI} (T_e=550 eV) conditions. In general, current drive is possible in the shadow region, however, the critical density is defined at $x > x_0$ and $y < y_{PI}$ in this case.

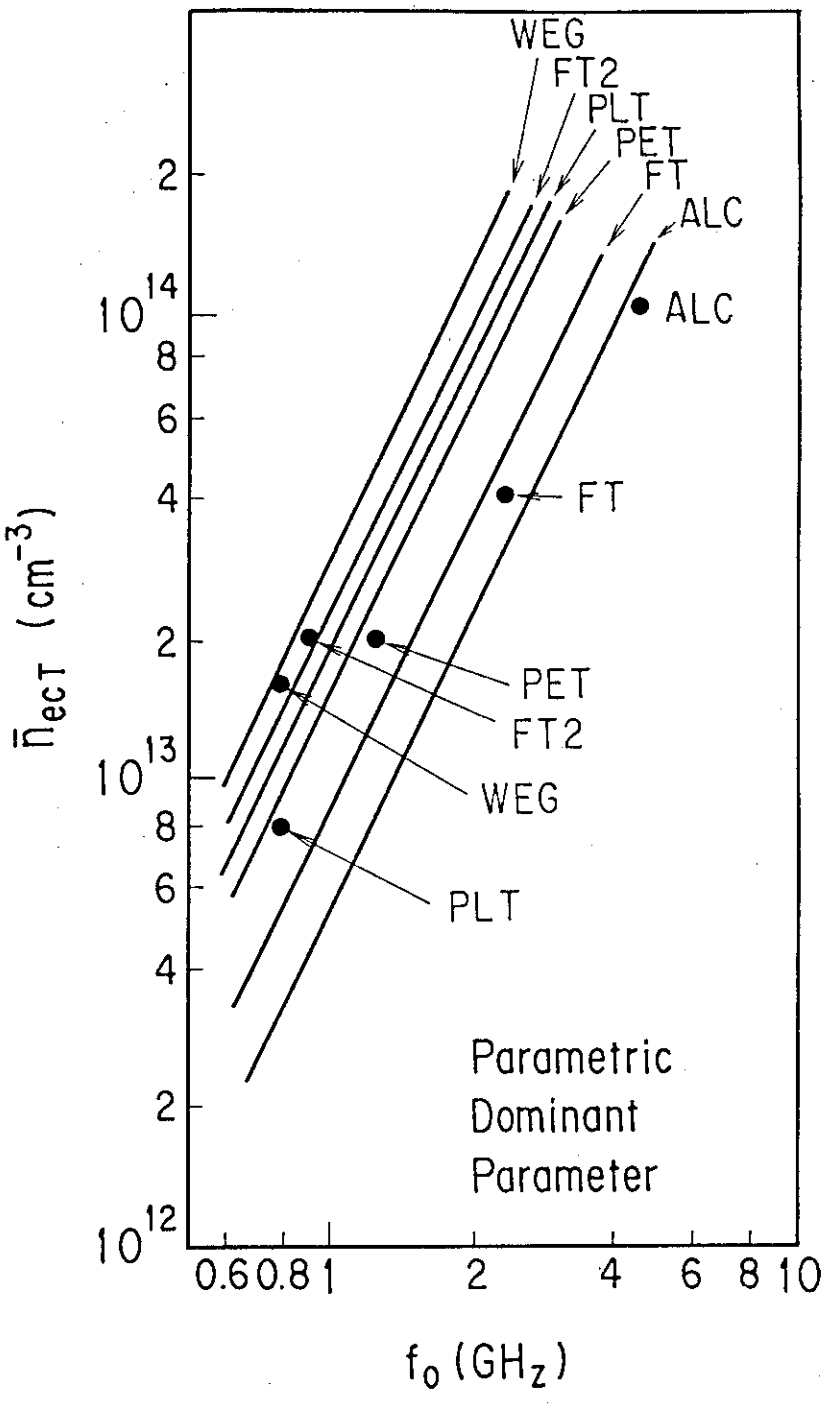

Fig. 4 The predicted and experimental critical density $\bar{n}_{ecT}$ and $\bar{n}_{ecX}$ are shown against f_0 for parametric dominant machines. Closed circles are experimental and the straight lines are predicted one, respectively.

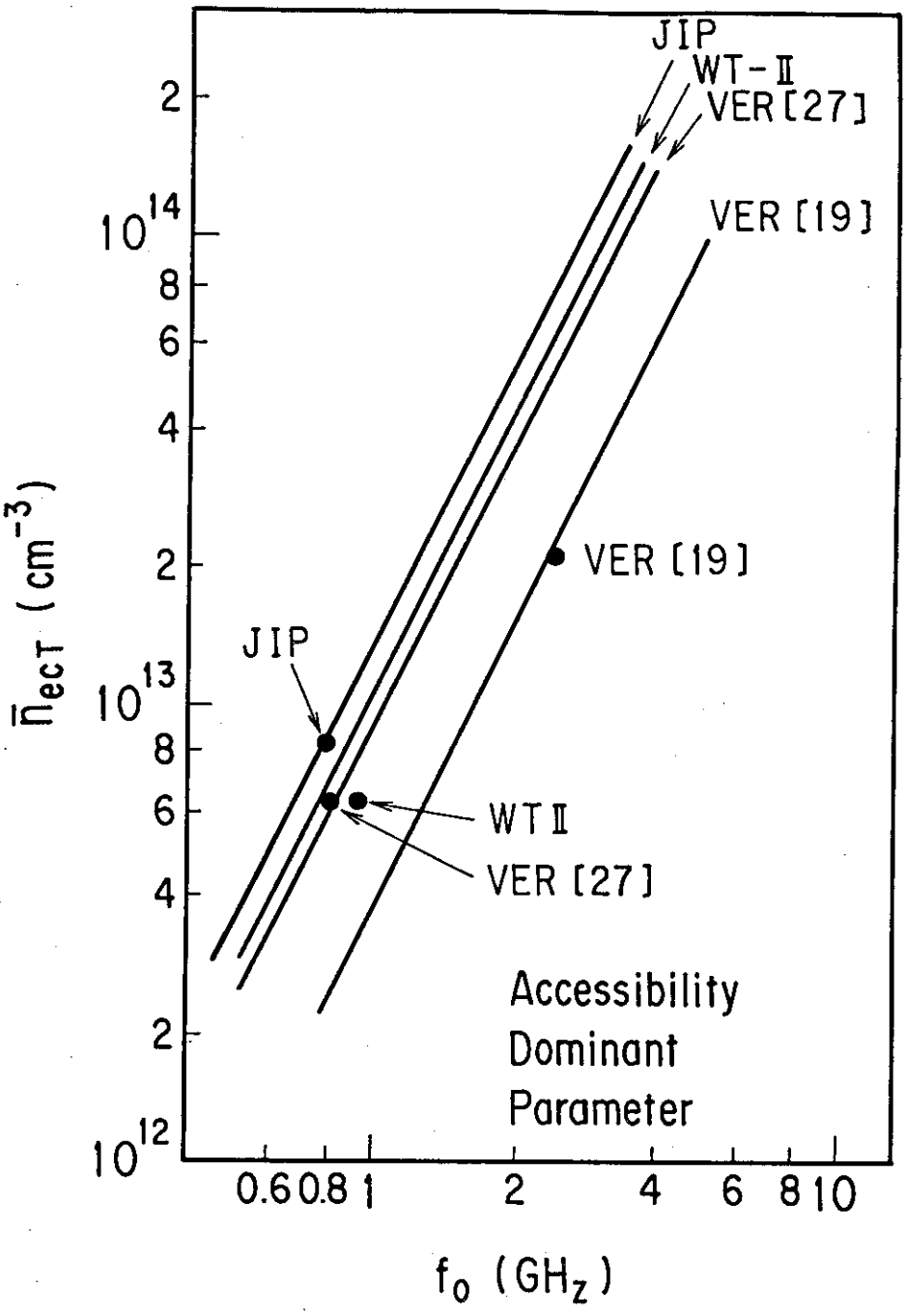

Fig. 5 The same one for the accessibility dominant parameters. Parentheses are the number of references.

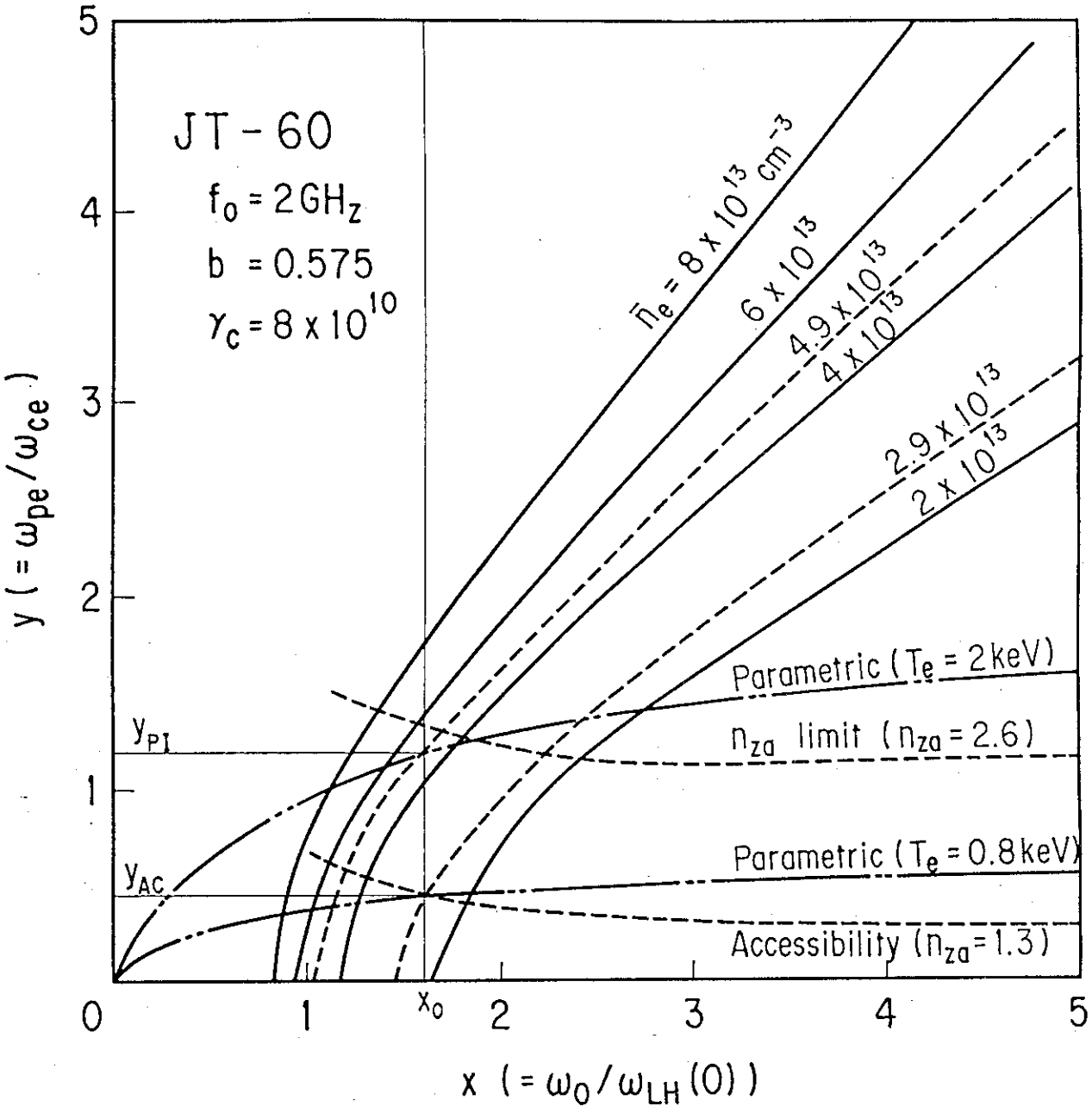

Fig. 6 Same graph as Fig. 3 for JT-60 case where n_{za}=1.3. Two cases are shown at high T_e (2 keV) and at low T_e (0.8 keV), respectively and n_{za} indicates the upper limit of rf spectrum. It is impossible for the current drive to be above n_{za}.

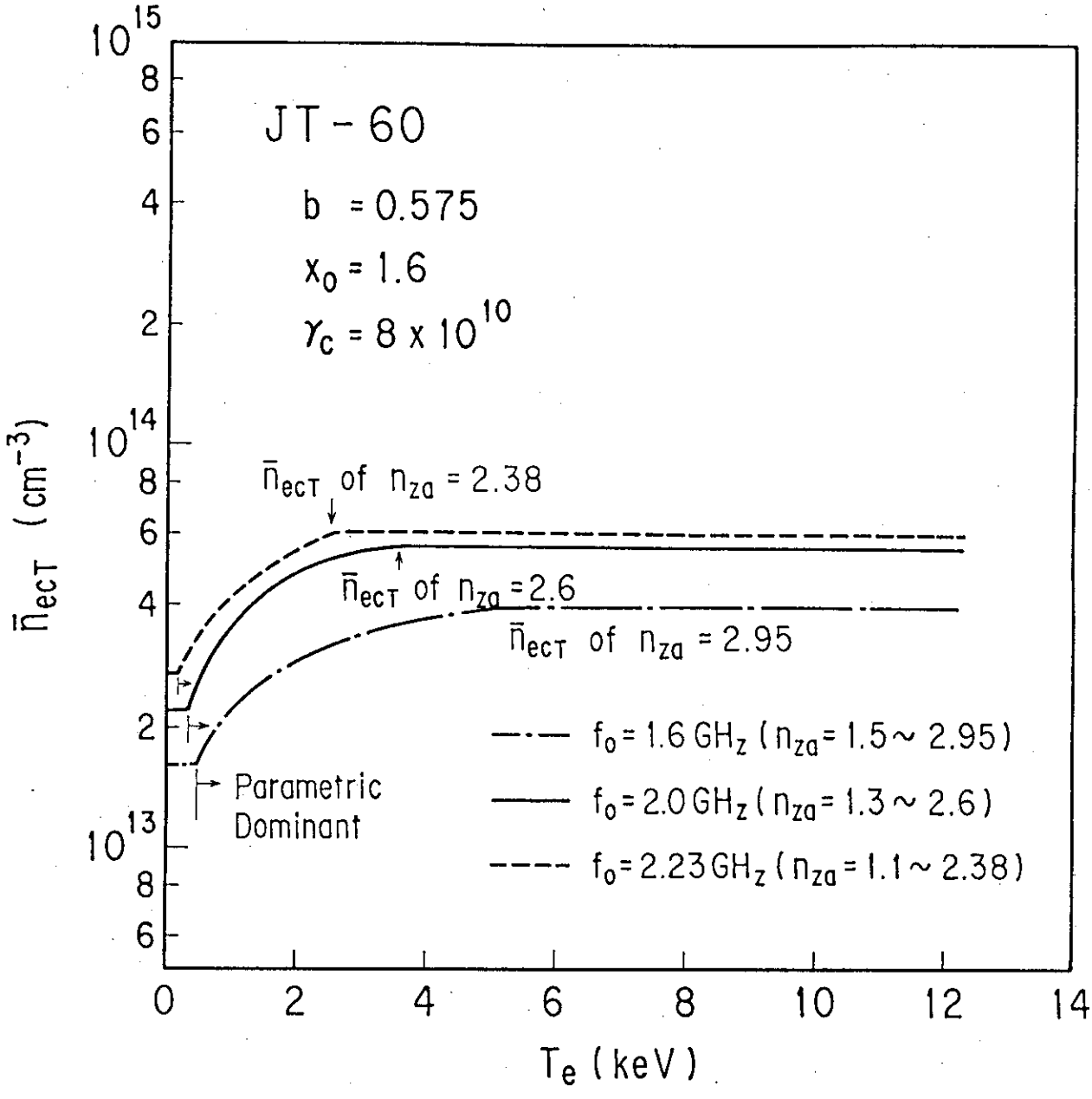

Fig. 7 The value of $\bar{n}_{ecT}$ vs T_e with f_0 as a parameter in JT-60 case. When T_e is lower than a critical one the current drive is in the accessibility dominant region and when T_e is larger than a critical one, the current drive is in the parametric dominant region. Even if, T_e becomes relatively larger $\bar{n}_{ect}$ is limitted a certain value due to the upper limit of rf spectrum.